Heat Carbonization and ZnCl2 Functionalization of Date Stone as an Adsorbent: Optimization of Material Fabrication Parameters and Adsorption Studies

Nesrine Abderrahim
Université de Gabès: Universite de Gabes
Ibtissem Boumnijel
Université de Gabès: Universite de Gabes
Hédi Ben Amor
Université de Gabès: Universite de Gabes
Ridha Djellabi (ridha.djellabi@yahoo.com)
University of Milan: Universita degli Studi di Milano https://orcid.org/0000-0002-1475-5565

Research Article

Keywords: Adsorbent synthesis optimization, Valorisation of agriculture wastes, Water remediation, Surface activation, Adsorption technology transfer, Response surface methodology

Posted Date: November 23rd, 2021

DOI: https://doi.org/10.21203/rs.3.rs-1042636/v1

Heat carbonization and $ZnCl_2$ functionalization of date stone as an adsorbent: optimization of material fabrication parameters and adsorption studies

Nesrine Abderrahim[1] , Ibtissem Boumnijel[2], Hédi Ben Amor[1], Ridha Djellabi[3,*]

[1]*University of Gabes, National Engineering School of Gabes (ENIG), RL Processes, Energetic, Environment and Electric Systems (PEESE), Gabes 6072, Tunisia.*

[2]*Laboratoire LMEEVED, Research and Technology Center of Energy, (CRTEn), Borj Cedria-Hammam Lif, TUNISIA.*

[3]*Department of Chemistry, Università degli Studi di Milano, via Golgi 19, 20133 Milano, Italy*

Corresponding author: R. Djellabi (ridha.djellabi@yahoo.com)

Graphical abstract

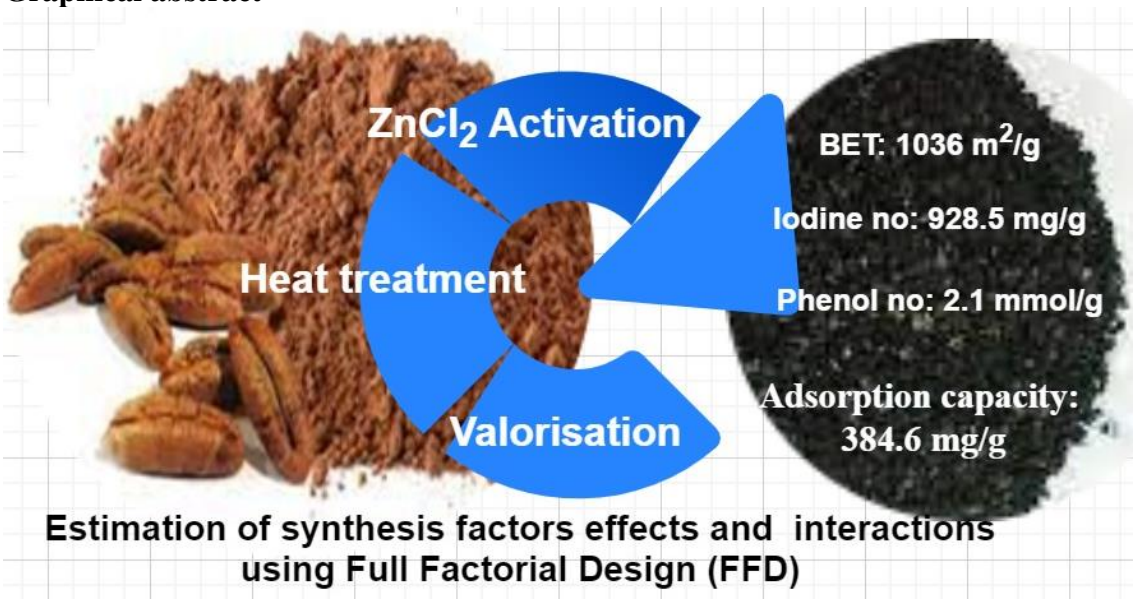

Abstract

The scientific community gave a lot attention to prepare adsorbents from different natural agriculture-based materials to be used alternative to commercial activated carbon. However, less studies on the optimization of fabrication parameters to obtain activated carbon with highly surface area and adsorption capacity. Herein, we report the synthesis conditions optimization of adsorbent based on date stone and modified with $ZnCl_2$. To obtain a highly adsorption ability of the materials, three systematic parameters were evaluated such as the activation temperature, activation time and the functionalization ratio by $ZnCl_2$. The optimization study showed that the best factors to fabricate an adsorbent from date stone are 700°C, 120 min and 2.0 (g/g), wherein, the specific surface area was found to be 1036 m^2/g. While, the iodine and phenol numbers were 928.5 mg/g and 2.1 mmol/g, respectively. To further understand the effect of synthesis parameters, the raw and the as-synthesized activated carbon were characterized via Fourier transmission infrared spectroscopy (FT-IR), X-ray diffraction (XRD), differential thermal analysis (DTA) and differential scanning calorimetry (DSC). Batch sorption tests to remove MB from water showed a maximum adsorption capacity of 384.6 mg/g using the prepared activated carbon at pH 6 and room temperature (25±2 °C). It was found also that the kinetic adsorption data obeyed the pseudo-second order and, both external diffusion and intra-particle diffusion control the adsorption. Based on the obtained results, the optimization of synthesis conditions through experimental and mobilization studies may help the transfer of technology in terms of agriculture-based materials valorisation towards the environmental remediation.

Keywords: Adsorbent synthesis optimization; Valorisation of agriculture wastes; Water remediation; Surface activation; Adsorption technology transfer; Response surface methodology.

1. Introduction

The recent huge socio-agro-industrial revolution development has led to an eco-system and environmental disequilibrium as a result of the huge irregular liquid, solid and gas pollution discharged in our planet. It became an inevitable to create novel ideas and find solutions to the existing problems. The scientific and health communities are recommending to apply green and clean technologies for the production processing, that respecting our environment from one side and the economic issues from another side. The management of wastes or recycling of materials are considered as clean approaches for better future of our planet. The exploitation of low-cost abundant or/and undesirable materials for different applications should be implemented into reality. The valorisation of agricultural and industrial wastes for the environmental remediation has received a huge attention recently from both the scientific and industrial communities (Nazir, Rehman, and Park 2021; Djellabi, Yang, Sharif, et al. 2019; Photiou and Vyrides 2021; Djellabi, Yang, Xiao, et al. 2019). Of these materials, the fabrication of adsorbents from natural materials and wastes to be used alternatively to commercial activated carbon have been over-addressed (Robles-Jimarez et al. 2022; Dabagh et al. 2021; Figueroa Campos et al. 2021; Negroiu et al. 2021). The valorisation of agro-wastes has two main advantages, the first is the reduction of solid pollution and waste management in the environment, and the second is the economic value of obtained adsorbents due to the local availability of several raw agro-materials (K Ramakrishnan et al. 2021). In this way, sustainable development goals (set by the General Assembly of the United Nations) are achieved (Kumar and Bhattacharya 2021). One of the main steps to transfer the use of agriculture-industrial based wastes to real world is the successful valorisation and modification of materials. To obtain a highly adsorptive ability, several properties should be obtained such as the porosity, functional surface, charge of the surface, external and internal surface area and so on. The synthesis conditions including the calcination temperature, time, and chemical oxidation/functionalization are the main factors

92 governing the above-mentioned properties. It is important to mention that the chemical
93 functional of the adsorbent surface influences directly the fixation of different pollutant species
94 due to the changing in surface charge, hydrophobicity and polarity. Two common ways are
95 applied to modify the surface of adsorbents, the first is the physical activation which involves
96 the direct heating of the materials in air or CO_2 stream, and the second is the chemical
97 functionalization of the surface using different KOH (Yuan et al. 2022), H_3PO_4 (Liu, Cheng,
98 and Wu 2021) and $ZnCl_2$ (Fakhar et al. 2021).

99 The co-treatment of adsorbents by heating and chemical activation can enhance cooperatively
100 the surface properties and surface area. However, choosing the right conditions in terms of
101 temperature of calcination vs time, and the type of chemical agent and its ratio are very
102 important to produce ideal adsorbents that are comparable to commercial ones.

103 Valorised date stone waste has showed great adsorptive capacity towards the removal of
104 different pollutants from water and wastewaters. Several physical and chemical modifications
105 have been reported to improve the adsorption capacity of date stone-based adsorbents (Daniel,
106 Gulyani, and Prakash Kumar 2012; Wakkel, Khiari, and Zagrouba 2019; Khelaifia et al. 2016).
107 In terms of surface specific surface area, some previous studies reported relatively high values
108 using different routes of activation, e.g., thermal/microwave activation (669.3 m2/g) (Hijab,
109 Parthasarathy, et al. 2021), date stone treated by H_3PO_4 (909 m^2/g) (Hijab, Saleem, et al. 2021),
110 activated with H_3PO_4 (900 m^2/g) (Boudia et al. 2019), date stone activated by pyrolysis/$ZnCl_2$
111 (1061 m^2/g) (Cherik and Louhab 2017).

112 As the production of highly adsorptive date stone-based adsorbent depends on several factors,
113 the optimization of fabrication conditions is very recommended. In the case of physical
114 activation, the heating condition per time is an important parameter to be evaluated. On the
115 other hand, in the context of chemical activation, the ratio of chemical agents influences directly
116 the surface charge, however, a high ratio may block the pores of the materials, therefore, the

ratio should be investigated. In the present study, the optimization of activation parameters (thermal and chemical) was investigated experimentally and also using planning experiments method via design expert. By the use of a such software and based on the experimental data (Sulaiman et al. 2018), a better optimization can be obtained which further facilities the large-scale synthesis processing and the transfer of the use agro-wastes technology to real-world application. Three parameters were controlled to fabricate the activated carbon from date stone waste such as temperature, time and the ratio of $ZnCl_2$. The as-prepared activated carbon-based adsorbent was characterized using several techniques to evaluate the morphology and structural proprieties. The sorption ability was evaluated to adsorb methylene blue in batch system.

2. Material and methods

2.1. Preparation of the activated carbon

The raw material (date stones) was obtained from a local date manufactory. Firstly, date stones were washed several times with water and distilled water, and dried at 105 °C for 24 h. After that, the raw material was mechanically crushed and particles with size of about 300 μm were recovered by sieving. The activation of date stones powder was carried out by controlling three parameters: values of calcination (400 and 700°C), time of calcination (30 and 120 min) and ratio of $ZnCl_2$ (0.25 and 2 w/w). The planification of preparation experiments were studies and optimized using 2^3 full factorial design (FFD) software in order to identify the role of applied parameters as a function of the adsorption capacity of MB as shown in **Table 1**.

Date stones powder was impregned in $ZnCl_2$ solution with different ratio (w/w) for 24 h at 110°C. After that, the sample is transferred to a furnace and heated at different temperature and time under a constant N_2 (99.99%) flow rate of 120 cm^3 / min. The obtained activated and then hot distilled water until the pH of the washed solution reached a value around 7. Finally, the sample were dried at 110°C for 24 h, ground and sieved to get a particle size of around 125 μm.

2. 2. Experimental design

142 In order to optimize the preparation of activated carbon, full factorial design was used with 2^3
143 tests, in total 8 experiments. The basic factorial was used in this study because the response
144 must be linear. For each factor, two extreme values were chosen delimiting the experimental
145 domain. The value -1 corresponds to low levels whereas +1 for high levels. During the
146 preparation of the activated carbon, the levels and ranges of the studied variables (A: activation
147 temperature, B: activation time and C: impregnation ratio) affecting MB removal are given in
148 Table 1. Response for MB adsorption capacity was used to develop an empirical model using
149 Design Expert 12 which correlates the response to the three independent variables. The general
150 mathematical model using the factorial design is expressed as follows (Özbay et al. 2013):

151 $$Y= b_0 + b_1A + b_2B + b_3C + b_4AB + b_5AC + b_6BC + b_7ABC \quad \text{(Eq.1)}$$

152 Where Y is the response , b terms are the parameters to be determined, b_0 is the global mean
153 and b_i represents the other regression coefficients.

154 *2. 3. Characterization of materials*

155 The structural of raw date stones (DS) and date stones activated carbon (DSAC) were
156 characterized via X-ray diffraction (XRD) with a Panalytical Xpert-PRO diffractometer with
157 monochromatic CuKα radiation (λ=1.54056 Å). Fourier transmission infrared spectrum of
158 DSAC was recorded on Nexus de ThermoFisher. The morphology of DS and DSAC was
159 analyzed using SEM- ZEISS EVO HD-15. The specific surface area was determined by the
160 BET (Brunaeur –Emmet–Teller) method using the adsorption–desorption isotherm of N_2 at 77
161 K. Before measuring the isotherm, the DSAC was degassed for 24 hours at 200 °C in order to
162 remove any moisture and impurities fixed at the sample surface.
163 The Iodine number (I_2 (mg/g)) was determined according to the ASTM D4607-94 method (D-
164 94 2006). In fact, it is a measure of the activated carbon micropore content (up to 2 nm) and it
165 provides an indication about the activated carbon capability to adsorb small molecular

compounds. The Phenol number (C_6H_5OH (mmol/g)) was measured using the method described by Ruiz Bevla et al (Ruiz Bevia, Prats Rico, and Marcilla Gomis 1984).

2.2.4. Batch adsorption studies

The effects of main variables governing the removal efficiency of MB such as solution pH, contact time, initial dye concentration and activated carbon dose were investigated in batch mode. A known quantity of the DSAC, prepared at the optimal conditions, was introduced into 500 mL of MB solution. The obtained mixture was stirred magnetically at 200 rpm and at room temperature (25±2°C). At different time intervals, the suspensions were filtered using micropore filter (0.2µm); then the filtrates were analysed for determining the residual concentration of MB solution using a visible spectrophotometer (HACH DR/2000) at the wavelength of 660 nm. The adsorption capacities q_t and q_e (mg/g) at a given time t and at equilibrium, respectively, as well as the removal efficiency (%) were computed according to the Equations (2) to (4).

$$q_t = \frac{(c_0 - c_t) \times V}{m} \quad \text{(Eq.2)}$$

$$q_e = \frac{(c_0 - c_e) \times V}{m} \quad \text{(Eq.3)}$$

$$\text{Removal efficiency}(\%) = \frac{(c_0 - c_t)}{c_0} \times 100 \quad \text{(Eq.4)}$$

Where c_0, c_t and c_e were the concentrations of MB (mg/L), at a given time t and at equilibrium, respectively. V is the volume of solution (L) and m the amount of the used DSAC (g).

3. Results and discussion

3.1. Optimization of the DSAC preparation conditions

The effects of synthesis factors and their interactions were invistigated by using full factorial design (FFD). As it can be seen from Table 1, DSAC samples prepared under different conditions were tested towards the adsorption of MB. We can deduce that the adsorption ability of DSAC samples depends significantly on the used operating parameters, and by varying the synthesis conditions, the adsorption capacity was found to be in the range of 40.48 to 318.02 mg/g.

Table 1. Dependence of activated carbon synthesis preparation factors and the yield of adsorbed MB.

Run Number	Activated carbon preparation variables			Adsorption capacity (mg/g)
	Activation temperature (°C)	Activation time (min)	Impregnation ratio (IR) (w/w)	
1	400	30	0.25	40.48
2	700	30	0.25	53.56
3	400	120	0.25	43.8
4	700	120	0.25	234.94
5	400	30	2.00	95.86
6	700	30	2.00	54.78
7	400	120	2.00	199.33
8	700	120	2.00	318.02

To estimate the positive and negative effects of different variables (calcination value, time of calcination and the ratio of impregnated $ZnCl_2$), a Pareto Chart (**Figure 1**) was developed based on the obtained results (shown in Table 1) using FFD calculation. The Pareto chart has two lines, namely Bonferroni and t- Value limit lines. It is important to point out that the factors with t-Values between Bonferroni and t-Value limit lines are likely to be significant (Shahryari, Goharrizi, and Azadi 2010; Bingöl, Saraydin, and Özbay 2015). From the Pareto chart, it can be deduced that the factor b (time of heating activation) is the main important factor for the fabrication of DSAC with high surface area and adsorption ability. The interaction AB is also very significant, wherein the calcination at 700°C for 120 min led to an excellent positive effect. In addition, the ratio of $ZnCl_2$ showed a great effect towards the activation of DSAC. Certainly, the heating activation is a main factor, together with $ZnCl_2$ activation as shown in Figure 1.a. The polynomial model equation, adopted in this study, is given as follows:

$$Y = 130.10 + 35.23A + 68.93B + 36.90C + 42.23AB - 15.83AC + 22.75BC \quad \text{(Eq.5)}$$

The positive sign in front of the terms indicates a synergetic effect, whereas a negative sign indicates an antagonistic effect (Karacan, Ozden, and Karacan 2007). It can be seen, from Equation 5, that the effects of the three studied variables are significant. Accordingly, the positive sign of the coefficients associated with the factors A, B and C points out that the increase of the activation time, temperature and impregnation ratio enhances the adsorption ability of DSAC towards the removal of MB. The quality of the developed model was evaluated based on the correlation coefficient (R^2) value. The closer the R^2 value to unity (0.995) , the better is the model. The validation of the method was performed through a comparison between the empirical and the actual values. Results are depicted in Figure 1.b. In Figure 2, at fixed ratio of $ZnCl_2$, the three-dimensional response surface showing the role of temperature and activation time is shown towards the adsorption of MB.

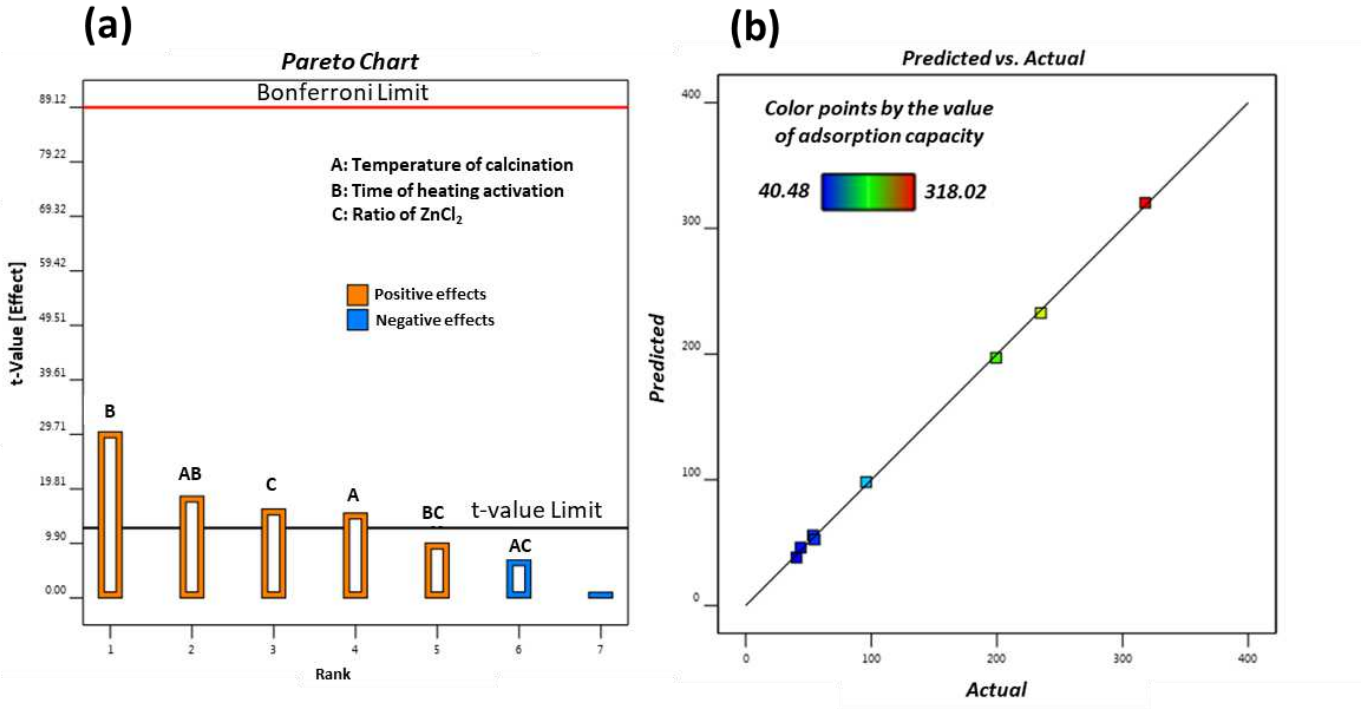

Figure 1. (a): Pareto Chart showing the main positive factors for a successful synthesis of DSAC. (b): Actual versus predicted values plot for the adsorption of MB on DSAC.

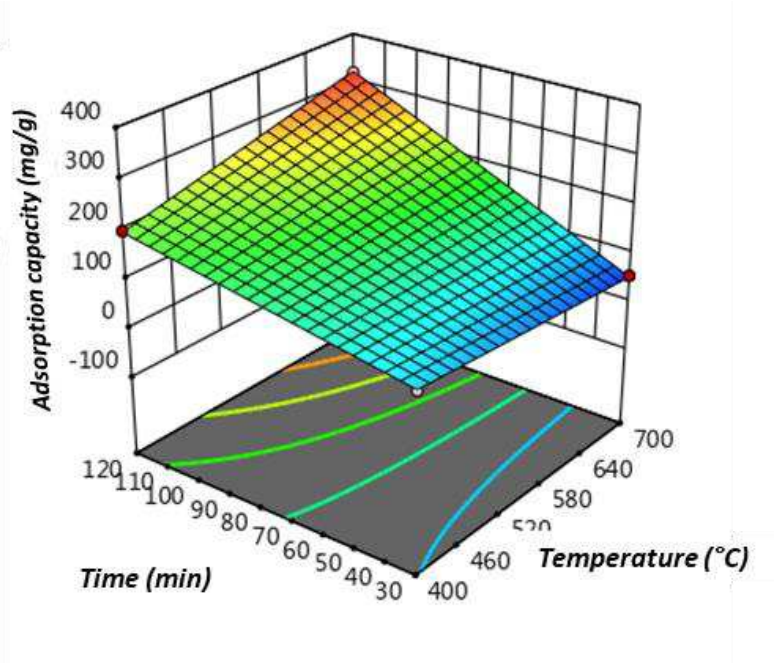

Figure 2. Response surface plot showing the effect of the temperature and activation time, at fixed ratio of impregnated $ZnCl_2$ (2 w/w).

3.2. Characterization of as-prepared activated carbon

Figure 3.a,b shows the SEM images of DS and DSAC. A notable change in the morphology of material after the heating treatment can be observed, wherein pores and channels of regular shapes were generated in the surface of DSAC, which in turn enhances the surface area of the material. Figure 3.c shows XRD patterns of raw DS and DSAC. Bare DS shows multi several diffraction peaks indicating its crystalline nature. However, the heat treatment has converted DS into AC carbon with amorphous nature. It can be seen in DSAC that there are two generated bands. The first is at (2θ = 20-30º) of C (002) diffraction which is due to amorphous carbon, and the second at around $2\theta = 43°$ as a result of graphite structure (Liu et al. 2010). Figure 3.d shows the FT-IR spectra of DSAC. The broad band at the interval of 3200-3400 cm^{-1} corresponds to the stretching vibration of the O-H functional groups. The characteristic bands of CH_2 and CH are detected at 2900 and 2650 cm^{-1}, respectively. The peaks at 1160 and 1050 cm^{-1} are consistent with alcoholic C-O (Djellabi, Yang, Wang, et al. 2019) and C-N stretching

238 vibrations (Soleimani and Kaghazchi 2014), respectively. The peak at 1560 cm^{-1} is assigned to
239 the stretching vibration of laconic groups C=O (Djellabi et al. 2020). The band at 1870 cm^{-1}
240 confirms the presence of carbonyl group (C=O) which is due to hemicellulose. The band at
241 2100 cm^{-1} is corresponding to the C≡C or/and C≡N stretching vibrations in the lignin, while the
242 strong peak at around 2360 cm^{-1} is due to isocyanate group of vibration (N=C=O) (Wang, Ding,
243 and Wang 2019). Figure 3.e,f shows BET N_2 adsorption/desorption isotherms of DSAC and its
244 pore diameter distribution, respectively. The surface area of DSAC was found to be 1036 m^2/g,
245 while DSCA shows micro sized pores. The results of DSAC characteristics in terms of surface
246 area, iodine number and phenol number are compared with some available commercial
247 activated carbon as listed in Table 2. It is worth to mention that the characteristics of as-prepared
248 DSAC are very similar to commercial activated carbon.

249 **Table 2.** Comparison of the characteristics of as-prepared DSAC with some commercial
250 activated carbons.

Material	SA (m^2/g)	I_2 (mg/g)	C_6H_5OH (mmol/g)
NORIT from Amersfoort, The Netherlands	950	1020	-
F-400 from Calgon Corp., Pittsburgh, PA	950	1000	-
UUB from China Carbon Corp.Taipei,Taiwan	980	1000	-
F400 from Chemviron	1050	1187	1.8
CECA	950	1094	1.7
PICAZINE	640	887	0.22
DSAC (this work)	1036	928.5	2.1

251

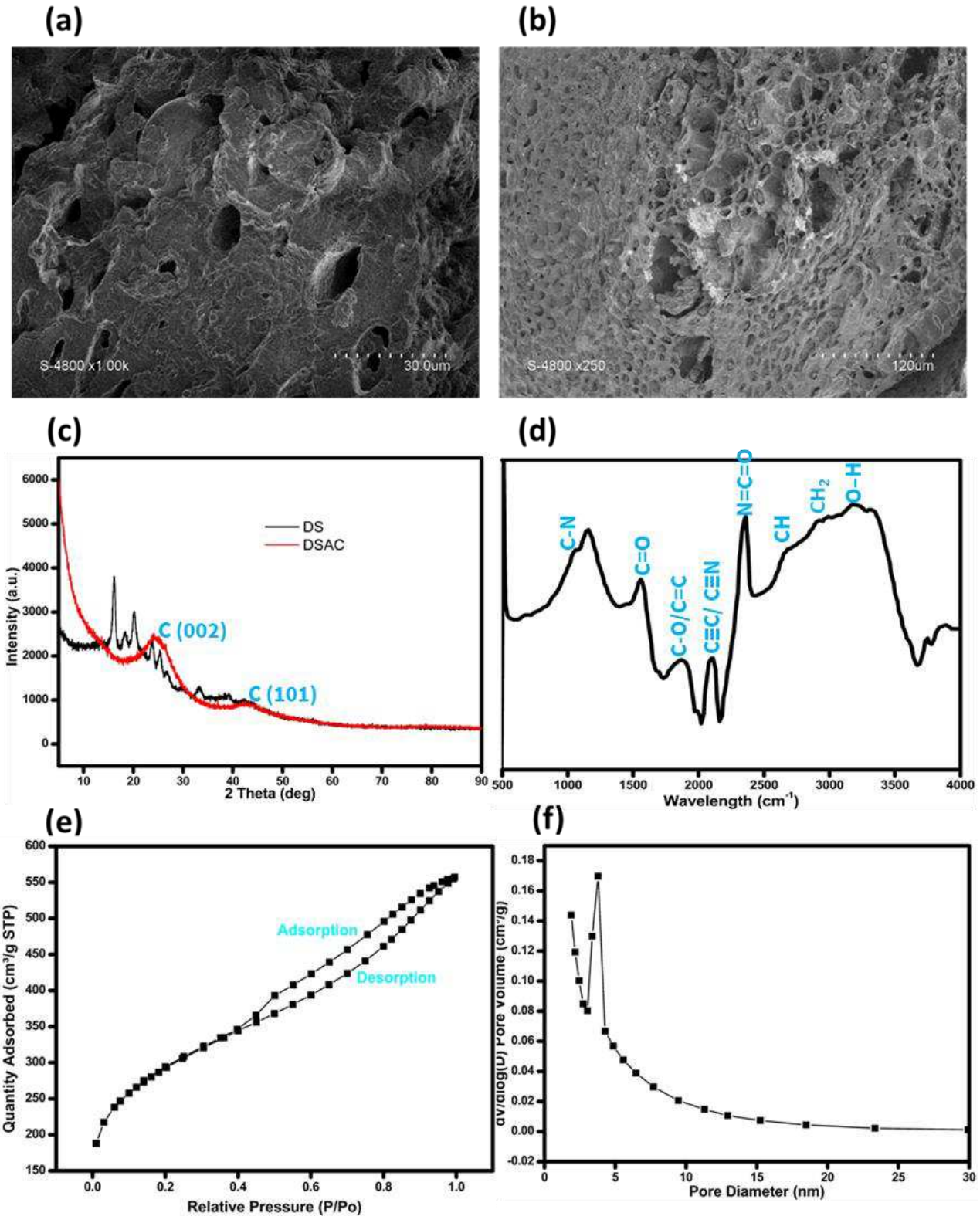

Figure 3. (a) and (b): SEM images of raw DS and as-prepared DSAC, respectively. (c): XRD spectra of raw raw DS and as-prepared DSAC. (e) and (f): BETadsorption-desoption isotherm and pore diamater of as-prepared DSAC, respectively.

3.3. Effect of operating parameters on the adsorption capacity

The capacity of adsorption of DSAC towards MB was studied from the range of 5 to 9 at a concentration of 83.5 ppm and a mass of DSAC of 0.2 g/L (**Figure 4.a**). The results showed that the capacity of adsorption was in the range of 321-313 mg/g at the pH range of 5-9. At this pH range, the charge of DSAC might be relatively negative within this pH range which allows the adsorption of MB molecules. To study the effect of the initial concentration of MB dye on the adsorption capacity at equilibrium time, a set of experiments was carried out at different concentrations varied from 50 to 185 mg/L. The quantity of DSAC was maintained at 0.2 g/L. As shown in Figure 3.b, the adsorption capacity increases from 204 to almost 318 mg/L when the initial MB concentration is increased from 50 to 83.5 mg/L. The higher the concentration, the higher the driving force to enhance the mass transfer from the solution to the adsorbent surface. Form the concentration of 80 to 180 ppm, the increase behaviour of adsorption capacity was found to be slower due to the saturation of adsorptive sites. The highest adsorption capacity was found to be 365 mg/g at 180 ppm. The effect of adsorbent mass, from 0.025 to 0.4 g/L, on the removal rate of MB at fixed concentration of MB (83.5 mg/L). As shown in Figure 4.c, the removal rate increases with the increase of adsorbent dose which is due to the availability of adsorptive sites as a function of the adsorbent dose.

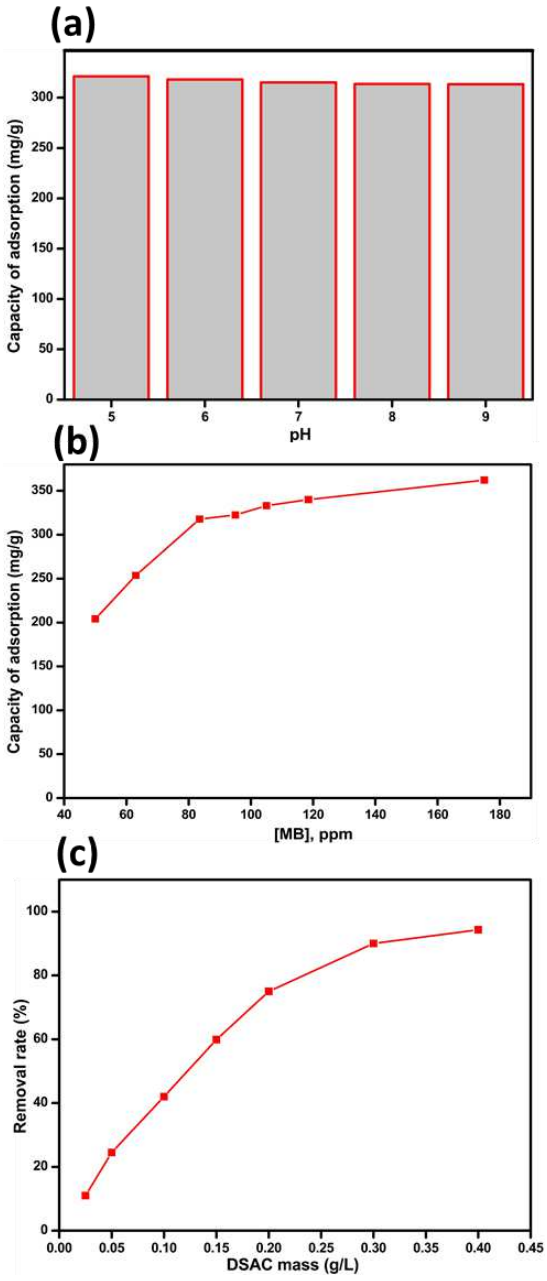

273

274 Figure 4. **(a)** Effect of pH solution of the adsorption capacity of DSAC, [MB] 83.5 ppm,
275 [DSAC] 0.2 g/L. (b) effect of MB concentration on the adsorption capacity, [DSAC] 0.2 g/L,
276 pH 6. (c) Effect of DSAC dose on the removal rate of MB, [MB] 83.5 ppm.

277 ***3.4. ADSORPTION ISOTHERMS STUDIES***

278 In order to study the isotherm adsorption of MB, a set of experiments was carried out by adding
279 0.2 g of the DSAC at different MB concentrations varied from 50 to 185 mg/L. The mixture
280 was stirred at room temperature until the equilibrium was reached. Three commonly used

isotherm models, Langmuir, Freundlich and Temkin have been applied to describe the mechanism of MB adsorption on the DSAC at the equilibrium state. Moreover, the applicability of the isotherm models, to fit the adsorption data, was evaluated by judging the correlation coefficients R^2 values. The linear Langmuir equation is given by Equation (6).

$$\frac{c_e}{q_e} = \frac{1}{q_m K_L} + \frac{c_e}{q_m} \quad \text{(Eq.6)}$$

Where q_e is the adsorbed amount (mg/g) and c_e is the dye concentration (mg/L) at the equilibrium state. q_m and K_L are Langmuir constants related to the maximum adsorption capacity (mg/g) and adsorption energy (l/mg), respectively. The Freundlich isotherm can be expressed by Equation 7. In fact, this model is an empirical equation based on adsorption phenomena occurring on the heterogeneous surface.

$$\log q_e = \log K_F + \frac{1}{n \log c_e} \quad \text{(Eq.7)}$$

Where K_F and n are the Freundlich constants that depend on the nature of the adsorbent. The Temkin isotherm has generally been applied in the linear form as presented by the Equations 8 and 9.

$$q_e = B_T \ln K_T + B_T \ln c_e \quad \text{(Eq.8)}$$

$$B_T = RT / b_T \quad \text{(Eq.9)}$$

Where T is the absolute temperature (K), R is the universal gas constant (8.314 J/mol K), b_T is the Temkin constant related to the adsorption heat (J/mg) and K_T is the equilibrium constant corresponding to the highest binding energy (l/mg). The experimental data were fitted to the isotherm models. The graphical presentations are displayed in Figure 5 (a, b and c).

The slope and the intercept of each linear plot, presented, are used to compute Langmuir, Freundlich, and Temkin parameters listed in Table 3 together with the associated correlation

coefficients. It can be seen that the correlation coefficient R^2 of Langmuir equation (R^2 = 0.9991) is higher than those of Freundlich (R^2 = 0.956) and Temkin (R^2 = 0.8713) equations. Hence, it seems that the adsorption isotherm data are well described by the Langmuir model which can be attributed to the homogeneous distribution of the active sites on the DSAC surface. The monolayer adsorption capacity, according to the Langmuir isotherm, is found to be 384.6 mg/g at 25°C. Furthermore, the value of 1/n gives by Freundlich assessed as 0.0778 proves the efficiency of the MB adsorption.

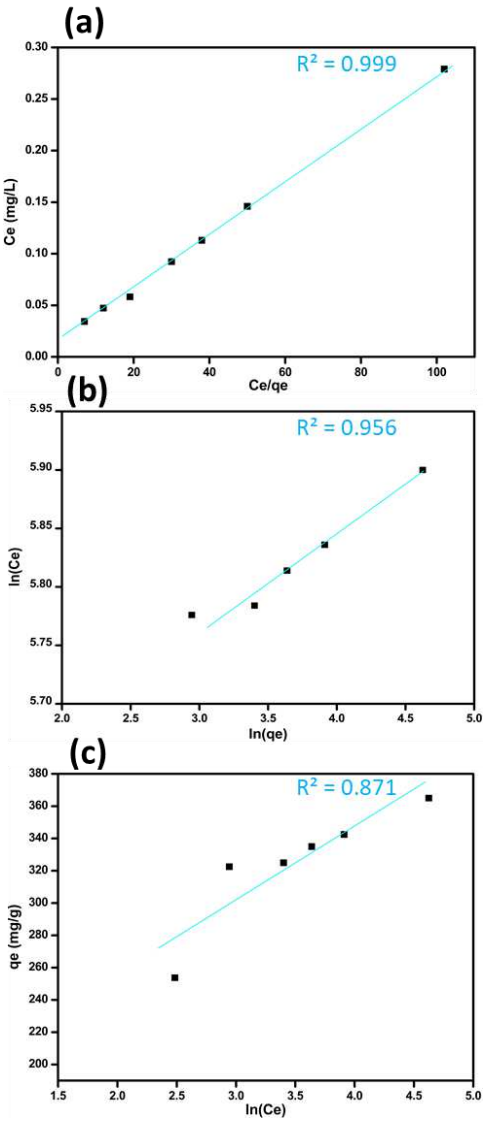

Figure 5. Presentation of Langmuir, Freundlich and Temkin isotherm models.

Table 3. Langmuir, Freundlich and Temkin isotherm constants and correlation coefficients for adsorption of MB onto the DSAC.

Langmuir isotherm			Freundlich isotherm			Temkin isotherm		
q_m (mg/g)	K_L(l/mg)	R^2	K_F (mg/g)	1/n	R^2	b_T (J/mg)	K_T (l/mg)	R^2
384.6	0.183	0.9991	253.1	0.0778	0.956	42.08	6.904	0.8713

3.5. ADSORPTION KINETIC STUDIES

To investigate the adsorption mechanism of the MB on the DSAC, kinetic models such as the pseudo –first order, the second order and the intra-particle diffusion were applied to study the adsorption dynamics. The pseudo-first-order kinetic model equation, expressed in linear form, is defined by Equation 10.

$$ln(q_e - q_t) = \ln q_e - k_1 t \quad \text{(Eq.10)}$$

Where q_e and q_t (mg/g) are the MB adsorbed amount at equilibrium and at time t (min), respectively. k_1 (l /min) is the pseudo-first-order rate constant.

The pseudo-second-order kinetic equation is described using Equation 11.

$$\frac{t}{q_t} = \frac{1}{k_2 q_e^2} + \frac{t}{q_e} \quad \text{(Eq.11)}$$

Where k_2 (g/mg. min) is the pseudo-second-order rate constant.

Spah and Schlunder model, given by Equation 12, is chosen to describe the external diffusion on the adsorbent.

$$\ln \frac{c_t}{c_0} = -k_{ext} t \quad \text{(Eq.12)}$$

Where k_{ext} is the external diffusion coefficient and C_t is the concentration at time t.

The intra-particle diffusion model is expressed by Equation 13.

$$q_t = K_p t^{1/2} + C \quad \text{(Eq.13)}$$

Where K_p is the intra-particle diffusion rate constant (mg/g. min $^{0.5}$) and C is the constant related to the thickness of the boundary layer (the intercept). In fact, the greater the value of this constant, the higher is the effect of the boundary layer.

334 The slope and the intercept values of each linear plot are listed in Table 4.

335 **Table** 4**.** Pseudo-first-order, pseudo-second-order, external diffusion and intra-particle
336 diffusion rate constants.

$q_{e,exp}$ (mg/g)	Pseudo-first-order			Pseudo-second-order			External diffusion		Intra-particle diffusion		
	$q_{e,cal}$ *(mg/g)*	k_1 *(1/min)*	R^2	$q_{e,cal}$ (mg/g)	k_2 (g/mg. min)	R^2	k_{ext} (min^{-1})	R^2	K_p ($mg/g.min^{0.5}$)	C (mg/g)	R^2
322.5	245.57	0.0189	0.939	333.33	0.000132	0.997	0.0128	0.9953	3.5715	250.68	0.8539

337 $q_{e,exp}$: the experimental adsorbed amount (mg/g)

338 $q_{e,cal}$: the calculated adsorbed amount (mg/g)

339 From Table 4, it can be deduced that the correlation coefficient R^2 value obtained from the
340 pseudo second-order (R^2=0.997) is significantly higher than that related to the pseudo-first-
341 order (R^2=0.939). In addition, the adsorbed amount $q_{e,cal}$ computed using the pseudo-second-
342 order kinetic model seems to be in good agreement with the experimental value $q_{e,exp}$. This
343 result suggests that the adsorption data fit well with the pseudo-second-order kinetic model.
344 The values of k_p and k_{ext} obtained respectively from external and intra-particle diffusion models
345 are listed in Table 4 with their correlation coefficient values. It was concluded that the
346 adsorption of MB on the surface of DSAC was achieved through two steps, the first step (during
347 the first 90 min) fits with the external diffusion, while the second step, after 90 min, was in
348 agreement with the intra-particle diffusion, which involves the insertion of MB molecules.

349 ***3.6 Comparison of DSAC with others adsorbents***

350 Table 5 lists the adsorption performances of previously reported studies in terms of activated
351 carbon fabrication from different raw materials under different conditions in comparison with
352 the as-prepared DSAC. In can be seen that, out of the mentioned adsorbents, DSAC showed a
353 great performance in terms of adsorption capacity, which proves the successful fabrication of
354 highly sorptive activated carbon from available a local availably agriculture waste.

355 **Table 5.** Comparison of activated carbons prepared from various raw materials and the
356 optimum conditions of MB removal.

Raw material	Preparation conditions	q_m (mg/g)	Reference
Pea Shells	IR=2, T=500°C for 1 hr.	246.91	(Geçgel, Özcan, and Gürpınar 2013)
Date stones	IR=0.5, T=600°C for 2hr.	286.3	(Alhamed 2006)
Groundnut shell	IR=1.75, T= 650°C for 15 min.	238	(Malik, Ramteke, and Wate 2006)
Walnut shells	IR=2, T= 450°C for 1hr.	315	(Yang and Qiu 2010)
Thevetia peruviana wood	IR=10%, T=400 and 800°C for 10 min.	98	(Baseri, Palanisamy, and Sivakumar 2012)
Tea fruit peel residues	IR=1, T=500°C for 40 min.	291.5	(Gao, Kong, et al. 2013)
Corn Husk Carbon	IR=1, T=500°C for 5 hr.	462.96	(Khodaie et al. 2013)
Biomass, Cartons and Polystyrene	IR=1, T=200°C for 2 hr	100	(Alothman, Habila, and Ali 2011)
Sindora Siamensis seed	IR=1-2, T=600°C for 3 hr	672.6	(Srisa-Ard 2014)
Waste carbon powder	IR=1, T=550°C for 1.5 hr	154	(Zaini et al. 2014)
Tea seed shells	IR=1, T=500°C for 1 hr	324.7	(Gao, Qin, et al. 2013)
Euphorbia antiquorum (L) wood	IR=10%, T=400 and 800°C for 10 min.	275	(Palanisamy and Sivakumar 2008)
Cassava peels	IR=7.5, T=200°C for 30 min	27	(Ilaboya et al. 2013)
Posidonia oceanica (L.) dead leaves	IR=45% T=600°C for 2 hr.	270.3	(Dural et al. 2011)
Date Stones	IR=2, T= 700°C for 2 hr.	384.6	This work

4. Conclusions

The present study shows that activated carbon prepared from date stones can be used as a good adsorbent. The methylene blue dye was employed as a molecule model to estimate the porosity and evaluate the adsorption aptitude of the synthesized DSCA. The optimal activated carbon was obtained using preparation conditions of 700 °C activation temperature, 120 min activation time and 2 impregnation ratio. Such conditions allow to obtain an activated carbon with high surface area comparable to commercial ones. The equilibrium data were analysed using the Langmuir, Freundlich and Temkin isotherm models. The Langmuir model was found to be the

best with a maximum adsorption capacity of 384.6 mg/g. Besides, it was found that the adsorption kinetics obeyed the pseudo-second order and; the intra-particle diffusion was not considered as the only rate controlling step. The iodine number value and maximum adsorption capacity of MB onto the synthesized DSCA showed that DSCA was capable of removal small and large environmental pollutants. According to the obtained results, it can be said that the DSCA could be employed as a low-cost alternative to commercial activated carbon for adsorption in the fixed-bed column system and in other industrial applications.

Authors Contributions: Nesrine Abderrahim: Methodology, Investigation, Writing - original draft; Ibtissem Boumnijel: Methodology, Investigation, writing; Hédi Ben Amor: Supervision, conceptualization and review; Ridha Djellabi: Writing - review & editing.

Ethics approval: Not applicable.

Consent to participate: Not applicable.

Consent to publish: Not applicable.

Competing interests: The author declares no competing interests.

Availability of data and materials: Not applicable.

Acknowledgments: The authors acknowledge the financial support of the Ministry of Higher Education (Tunisia).

Availability of data and materials: Not applicable.

References

Alhamed, Yahia A. 2006. 'Activated carbon from dates' stone by ZnCl2 activation', *JKAU Eng Sci*, 17: 5-100.

Alothman, Z, M Habila, and R Ali. 2011. 'Preparation of activated carbon using the copyrolysis of agricultural and municipal solid wastes at a low carbonization temperature', *Carbon*, 24: 67-72.

Baseri, J Raffiea, PN Palanisamy, and P Sivakumar. 2012. 'Preparation and characterization of activated carbon from Thevetia peruviana for the removal of dyes from textile waste water', *Advances in Applied Science Research*, 3: 377-83.

Bingöl, Deniz, Dursun Saraydin, and Dilek Şolpan Özbay. 2015. 'Full factorial design approach to Hg (II) adsorption onto hydrogels', *Arabian Journal for Science and Engineering*, 40: 109-16.

Boudia, Rabia, Goussem Mimanne, Karim Benhabib, and Laurence Pirault-Roy. 2019. 'Preparation of mesoporous activated carbon from date stones for the adsorption of Bemacid Red', *Water Science and Technology*, 79: 1357-66.

Cherik, Dalila, and Krim Louhab. 2017. 'Preparation of microporous activated carbon from date stones by chemical activation using zinc chloride', *Energy Sources, Part A: Recovery, Utilization, and Environmental Effects*, 39: 1935-41.

D-94, ASTM. 2006. 'Standard test method for determination of iodine number of activated carbon', *West Conshocken, PA: American Society for Testing Materials*.

Dabagh, Abdelkader, Abdellah Bagui, M'hamed Abali, Rachid Aziam, Mohamed Chiban, Fouad Sinan, and Mohamed Zerbet. 2021. 'Increasing the Adsorption Efficiency of Methylene Blue by Acid Treatment of the Plant Carpobrotus edulis', *Chemistry Africa*: 1-14.

Daniel, Veena Valsamma, BB Gulyani, and BG Prakash Kumar. 2012. 'Usage of date stones as adsorbents: a review', *Journal of dispersion science and technology*, 33: 1321-31.

Djellabi, Ridha, Bo Yang, Hafiz Muhammad Adeel Sharif, Juanjuan Zhang, Jafar Ali, and Xu Zhao. 2019. 'Sustainable and easy recoverable magnetic TiO2-Lignocellulosic Biomass@ Fe3O4 for solar photocatalytic water remediation', *Journal of Cleaner Production*, 233: 841-47.

Djellabi, Ridha, Bo Yang, Yan Wang, Xiaoqing Cui, and Xu Zhao. 2019. 'Carbonaceous biomass-titania composites with TiOC bonding bridge for efficient photocatalytic reduction of Cr (VI) under narrow visible light', *Chemical Engineering Journal*, 366: 172-80.

Djellabi, Ridha, Bo Yang, Ke Xiao, Yan Gong, Di Cao, Hafiz Muhammad Adeel Sharif, Xu Zhao, Caizhen Zhu, and Junmin Zhang. 2019. 'Unravelling the mechanistic role of TiOC bonding bridge at titania/lignocellulosic biomass interface for Cr (VI) photoreduction under visible light', *Journal of colloid and interface science*, 553: 409-17.

Djellabi, Ridha, Xu Zhao, Claudia Letizia Bianchi, Peidong Su, Jafar Ali, and Bo Yang. 2020. 'Visible light responsive photoactive polymer supported on carbonaceous biomass for photocatalytic water remediation', *Journal of Cleaner Production*, 269: 122286.

Dural, Mehmet Ulas, Levent Cavas, Sergios K Papageorgiou, and Fotis K Katsaros. 2011. 'Methylene blue adsorption on activated carbon prepared from Posidonia oceanica (L.) dead leaves: Kinetics and equilibrium studies', *Chemical Engineering Journal*, 168: 77-85.

Fakhar, Nida, Suhail Ayoub Khan, Weqar Ahmad Siddiqi, and Tabrez Alam Khan. 2021. 'Ziziphus jujube waste-derived biomass as cost-effective adsorbent for the sequestration of Cd2+ from aqueous solution: Isotherm and kinetics studies', *Environmental Nanotechnology, Monitoring & Management*, 16: 100570.

Figueroa Campos, Gustavo A, Jeffrey Paulo H Perez, Inga Block, Sorel Tchewonpi Sagu, Pedro Saravia Celis, Andreas Taubert, and Harshadrai M Rawel. 2021. 'Preparation of Activated Carbons from Spent Coffee Grounds and Coffee Parchment and Assessment of Their Adsorbent Efficiency', *Processes*, 9: 1396.

Gao, Jun-jie, Ye-bo Qin, Tao Zhou, Dong-dong Cao, Ping Xu, Danielle Hochstetter, and Yue-fei Wang. 2013. 'Adsorption of methylene blue onto activated carbon produced from tea (Camellia sinensis L.) seed shells: kinetics, equilibrium, and thermodynamics studies', *Journal of Zhejiang University Science B*, 14: 650-58.

Gao, Junjie, Dedong Kong, Yuefei Wang, Jing Wu, Shili Sun, and Ping Xu. 2013. 'Production of mesoporous activated carbon from tea fruit peel residues and its evaluation of methylene blue removal from aqueous solutions', *BioResources*, 8: 2145-60.

Geçgel, Ünal, Gülce Özcan, and Gizem Çağla Gürpınar. 2013. 'Removal of methylene blue from aqueous solution by activated carbon prepared from pea shells (Pisum sativum)', *Journal of Chemistry*, 2013.

Hijab, M, J Saleem, P Parthasarathy, HR Mackey, and G McKay. 2021. 'Two-stage optimisation for malachite green removal using activated date pits', *Biomass Conversion and Biorefinery*, 11: 727-40.

Hijab, Mouhammad, Prakash Parthasarathy, Hamish R Mackey, Tareq Al-Ansari, and Gordon McKay. 2021. 'Minimizing adsorbent requirements using multi-stage batch adsorption for malachite green removal using microwave date-stone activated carbons', *Chemical Engineering and Processing-Process Intensification*: 108318.

Ilaboya, IR, EO Oti, GO Ekoh, LO Umukoro, and Akanu Ibiam. 2013. 'Performance of activated carbon from cassava peels for the treatment of effluent wastewater', *Iranica Journal of Energy and Environment*, 4: 361-70.

K Ramakrishnan, Rohith, Vinod VT Padil, Stanisław Wacławek, Miroslav Černík, and Rajender S Varma. 2021. 'Eco-Friendly and Economic, Adsorptive Removal of Cationic and Anionic Dyes by Bio-Based Karaya Gum—Chitosan Sponge', *Polymers*, 13: 251.

Karacan, Filiz, Umit Ozden, and Süleyman Karacan. 2007. 'Optimization of manufacturing conditions for activated carbon from Turkish lignite by chemical activation using response surface methodology', *Applied Thermal Engineering*, 27: 1212-18.

Khelaifia, Fatma Zohra, Sabir Hazourli, Sana Nouacer, Hachani Rahima, and Mounir Ziati. 2016. 'Valorization of raw biomaterial waste-date stones-for Cr (VI) adsorption in aqueous solution: Thermodynamics, kinetics and regeneration studies', *International Biodeterioration & Biodegradation*, 114: 76-86.

Khodaie, Maryam, Nahid Ghasemi, Babak Moradi, and Mohsen Rahimi. 2013. 'Removal of methylene blue from wastewater by adsorption onto ZnCl2 activated corn husk carbon equilibrium studies', *Journal of Chemistry*, 2013.

Kumar, Abhishek, and Tanushree Bhattacharya. 2021. 'Biochar: a sustainable solution', *Environment, Development and Sustainability*, 23: 6642-80.

Liu, Hai, Cheng Cheng, and Haiming Wu. 2021. 'Sustainable utilization of wetland biomass for activated carbon production: A review on recent advances in modification and activation methods', *Science of The Total Environment*: 148214.

Liu, Xiao-Yan, Miao Huang, Hai-Long Ma, Zeng-Qiang Zhang, Jin-Ming Gao, Yu-Lei Zhu, Xiao-Jin Han, and Xiang-Yun Guo. 2010. 'Preparation of a carbon-based solid acid catalyst by sulfonating activated carbon in a chemical reduction process', *Molecules*, 15: 7188-96.

Malik, R, DS Ramteke, and SR Wate. 2006. 'Physico-chemical and surface characterization of adsorbent prepared from groundnut shell by ZnCl 2 activation and its ability to adsorb colour'.

Nazir, Ghazanfar, Adeela Rehman, and Soo-Jin Park. 2021. 'Valorization of shrimp shell biowaste for environmental remediation: Efficient contender for CO2 adsorption and separation', *Journal of environmental management*, 299: 113661.

Negroiu, Mihai, Anca Andreea Țurcanu, Ecaterina Matei, Maria Râpă, Cristina Ileana Covaliu, Andra Mihaela Predescu, Cristian Mircea Pantilimon, George Coman, and Cristian Predescu. 2021. 'Novel Adsorbent Based on Banana Peel Waste for Removal of Heavy Metal Ions from Synthetic Solutions', *Materials*, 14: 3946.

Özbay, N, AŞ Yargıç, RZ Yarbay-Şahin, and E Önal. 2013. 'Full factorial experimental design analysis of reactive dye removal by carbon adsorption', *Journal of Chemistry*, 2013.

Palanisamy, PN, and P Sivakumar. 2008. 'Production and Characterization of a novel non-conventional low-cost adsorbent from Euphorbia Antiquorum L', *Rasayan J Chem*, 1: 901-10.

Photiou, Panagiota, and Ioannis Vyrides. 2021. 'Recovery of phosphate from dewatered anaerobic sludge and wastewater by thermally treated P. oceanica residues and its potential application as a fertilizer', *Journal of environmental management*, 298: 113441.

Robles-Jimarez, HR, L Sanjuan-Navarro, N Jornet-Martínez, CT Primaz, R Teruel-Juanes, C Molins-Legua, A Ribes-Greus, and P Campíns-Falcó. 2022. 'New silica based adsorbent material from rice straw and its in-flow application to nitrate reduction in waters: Process sustainability and scale-up possibilities', *Science of The Total Environment*, 805: 150317.

Ruiz Bevia, F, D Prats Rico, and AF Marcilla Gomis. 1984. 'Activated carbon from almond shells. Chemical activation. 2. Zinc chloride activation temperature influence', *Industrial & engineering chemistry product research and development*, 23: 269-71.

Shahryari, Zohre, Ataallah Soltani Goharrizi, and Mehdi Azadi. 2010. 'Experimental study of methylene blue adsorption from aqueous solutions onto carbon nano tubes', *International Journal of Water Resources and Environmental Engineering*, 2147483647: 016-28.

Soleimani, Mansooreh, and Tahereh Kaghazchi. 2014. 'Low-cost adsorbents from agricultural by-products impregnated with phosphoric acid', *Advanced Chemical Engineering Research*, 3: 34-41.

Srisa-Ard, Samarn. 2014. 'Preparation of Activated Carbon from Sindora Siamensis Seed and Canarium Sublatum Guillaumin fruit for Methylene Blue Adsorption', *International Transaction Journal of Engineering, Management, & Applied Sciences & Technologies. ISSN*: 2228-9860.

Sulaiman, Nurul Syuhada, Rokiah Hashim, Mohd Hazim Mohamad Amini, Mohammed Danish, and Othman Sulaiman. 2018. 'Optimization of activated carbon preparation from cassava stem using response surface methodology on surface area and yield', *Journal of Cleaner Production*, 198: 1422-30.

Wakkel, Manel, Besma Khiari, and Fethi Zagrouba. 2019. 'Textile wastewater treatment by agro-industrial waste: equilibrium modelling, thermodynamics and mass transfer mechanisms of cationic dyes adsorption onto low-cost lignocellulosic adsorbent', *Journal of the Taiwan Institute of Chemical Engineers*, 96: 439-52.

Wang, Zuo, Yaoke Ding, and Jincheng Wang. 2019. 'Novel Polyvinyl Alcohol (PVA)/Cellulose Nanocrystal (CNC) supramolecular composite hydrogels: preparation and application as soil conditioners', *Nanomaterials*, 9: 1397.

Yang, Juan, and Keqiang Qiu. 2010. 'Preparation of activated carbons from walnut shells via vacuum chemical activation and their application for methylene blue removal', *Chemical Engineering Journal*, 165: 209-17.

Yuan, Min, Tianchang Liu, Qi Shi, and Jinxiang Dong. 2022. 'Understanding the KOH activation mechanism of zeolitic imidazolate framework-derived porous carbon and their corresponding furfural/acetic acid adsorption separation performance', *Chemical Engineering Journal*, 428: 132016.

Zaini, Muhammad Abbas Ahmad, Ting Chiew Ngiik, Mohd Johari Kamaruddin, Siti Hamidah Mohd Setapar, and Mohd Azizi Che Yunus. 2014. 'Zinc chloride-activated waste carbon powder for decolourization of methylene blue', *Jurnal Teknologi*, 67.